The 22nd Conference of Mechanical Engineering Network of Thailand
15-17 October 2008, Thammasat University, Rangsit Campus, Pathum Thani, Thailand

Adaptive Nodeless Variable Finite Element Method for Convectively-Cooled Solids

Sutthikom Puntimakornkij, Atipong Malatip and Pramote Dechaumphai*

Department of Mechanical Engineering, Chulalongkorn University,
254 Phyathai Road,Patumwan, Bangkok 10330, Thailand,
Tel: 0-2218-6621, Fax: 0-2218-6621 *E-mail: fmepdc@eng.chula.ac.th

Abstract

The adaptive nodeless variable finite element method for convectively-cooled solids is presented. The nodeless variable finite element method is developed for analyzing heat transfer in solids that is coupled with the flow in channels. The nodeless variable element employs quadratic interpolation functions to provide higher solution accuracy without requiring actual nodes. The coupled fluid/solid solution is further improved by incorporating an adaptive meshing technique. Several examples are presented to demonstrate the efficiency of the combined method.

Key words: Adaptive mesh, nodeless variable Finite element, convectively-cooled solids.

1. Introduction

Design and analysis of convectively-cooled solids are encountered in many practical engineering problems. Currently, the finite element method is widely used to solve for the temperature distribution in solids, as well as the behavior of the fluid flow [1-3]. The problem is more complicated when the coupled analysis is required to predict the solid and fluid behavior simultaneously. Such analysis is known as the conjugate heat transfer [4-5] that needs immense effort to solve the Navier-Stokes equations of the fluid. Recently, the nodeless variable finite element [6-7] has been developed to provide higher solution accuracy without requiring actual nodes. In addition, the solution accuracy can be further improved by using the adaptive finite element technique [3,6-7]. The technique generates small elements clustered in the high temperature gradient regions to provide accurate solution. Larger elements are generated in the other regions where the temperature is uniform to reduce the number of unknowns and computational time.

In this paper, an adaptive nodeless variable finite element method is developed to predict the temperatures in the solid and the fluid flowing in a channel. Convection heat transfer between the solid and fluid is included along the solid/fluid interface. For a fluid flow through a channel, the fluid analysis may be treated as one dimensional flow. In this case, the couple solid/fluid analysis can be simplified so that the computational effort is reduced significantly. Heat transfer in the fluid thus can be characterized by the fluid bulk temperature and the convection coefficient. The solid/fluid heat transfer is then coupled and their solutions can be solved simultaneously. The nodeless variable finite element is employed to improve the predicted temperature distribution. The nodeless variable finite element uses the quadratic interpolation functions to describe the temperature distribution over the element. The use of the nodeless variable finite element can also be referred to as a hierarchical methodology, since the element reduces to the standard linear element when the nodeless variables are constrained to zero or eliminated.

To further improve the predicted solution of the solid and fluid temperatures, an adaptive finite element technique has been incorporated. Examples are presented in the paper to demonstrate the efficiency of the proposed method. These examples are a convectively-cooled solid subjected to uniform heating and a plate with intense heating.

2. Theoretical formulation

2.1 Governing equations

The equations which govern convectively-cooled solids are the one-dimensional conservation of energy equation for the fluid flow, and the two-dimensional conservation of energy equation for the solid. These governing differential equations are,

Energy equation in fluid,

$$\rho_f c_f u_f A_f \frac{\partial T_f}{\partial x} - k_f A_f \frac{\partial^2 T_f}{\partial x^2} - hp\left(T_f - T_s\right) - Q_f A_f = 0 \tag{1}$$

Energy equation in solid,

$$k_s\left(\frac{\partial^2 T_s}{\partial x^2} + \frac{\partial^2 T_s}{\partial y^2}\right) - Q_s = 0 \tag{2}$$

where the subscript f and s are for the fluid and the solid, respectively; u is the velocity in x direction, ρ is the density, c is the specific heat, k is the coefficient of thermal conductivity, h is the convective heat transfer coefficient, p is the perimeter, Q is the internal heat generation rate per volume and T is the temperature.

2.2 Finite element formulation

The nodeless variable finite element equations are derived using the method of weighted residuals. The mass transport element and triangular element are employed in this study. For both elements, the distributions of temperature over the elements are assumed respectively in the form

$$T(x) = \sum_{i=1}^{3} N_i(x) T_i \tag{3}$$

$$T(x, y) = \sum_{i=1}^{6} N_i(x, y) T_i \tag{4}$$

where N_i consists of the element interpolation functions and T_i is the vector of the unknown temperatures and the nodeless variables. For the fluid, the nodal temperatures are T_1 and T_2, while T_3 is the nodeless variable. For the solid, the nodal temperatures are T_1 through T_3, while T_4 through T_6 are the nodeless variables. The element interpolation functions, N_1 and N_2 in fluid, N_1 through N_3 in solid are the standard two-node element and three-node triangular element, respectively while N_3 in fluid and N_4 through N_6 in solid are the nodeless variable interpolation functions. The interpolation functions implemented in this paper are,

For fluid,

$$N_1 = 1 - x/L$$
$$N_2 = x/L \tag{5}$$
$$N_3 = 4N_1N_2$$

For solid,

$$N_1 = L_1$$
$$N_2 = L_2$$
$$N_3 = L_3$$
$$N_4 = 4L_2L_3 \tag{6}$$
$$N_5 = 4L_1L_3$$
$$N_6 = 4L_1L_2$$

where L in eq. (6) is area coordinates [8-9].

$$L_i = (a_i + b_i x + c_i y)/2A \tag{7}$$

To derive the nodeless variable finite element matrices, the method of weighted residuals is first applied to Eqs. (1) and (2). Integration by parts is then performed using the Gauss theorem to yield the boundary terms for applying boundary conditions. The nodeless variable finite element equations are,

For fluid,

$$\int_0^L kA\left\{\frac{\partial N}{\partial x}\right\}\left\lfloor\frac{\partial N}{\partial x}\right\rfloor dx\{T_f\} + \int_0^L \dot{m}c\{N\}\left\lfloor\frac{\partial N}{\partial x}\right\rfloor dx\{T_f\}$$

$$+\int_0^L hp\{N\}\lfloor N\rfloor dx\{T_f\} - \int_0^L hp\{N\}\lfloor N\rfloor dx\{T_s\}$$

$$= \left(\{N\}kA\frac{\partial T_f}{\partial x}\right)\Bigg|_0^L + \int_0^L QA\{N\}dx \tag{8}$$

For solid,

$$\int_A kt\left(\left\{\frac{\partial N}{\partial x}\right\}\left\lfloor\frac{\partial N}{\partial x}\right\rfloor + \left\{\frac{\partial N}{\partial y}\right\}\left\lfloor\frac{\partial N}{\partial y}\right\rfloor\right)dA\{T_s\}$$

$$+\int_0^L hp\{N\}\lfloor N\rfloor dx\{T_s\} - \int_0^L hp\{N\}\lfloor N\rfloor dx\{T_f\}$$

$$= \int_\Gamma kt\{N\}\left(\frac{\partial T_s}{\partial x}n_x + \frac{\partial T_s}{\partial y}n_y\right)d\Gamma + \int_A Qt\{N\}dA \tag{9}$$

where A is the element cross-sectional area for fluid and the element area in solid, $\dot{m}$ is the mass flow rate, L is the element length, Γ is the element boundary, t is the element thickness, n_x and n_y are the direction cosines of the unit vector normal to the edge. The nodeless variable finite element matrices are,

For fluid,

$$\left([K_c] + [K_v] + [K_{f-s}]\right)\{T_f\} - [K_{f-s}]\{T_s\} = \{Q_{Q_f}\} \tag{10}$$

For solid,

$$\left([K_c] + [K_{f-s}]\right)\{T_s\} - [K_{f-s}]\{T_f\} = \{Q_{Q_s}\} \tag{11}$$

The above Eqs. (10) and (11) can be written together as,

$$\begin{bmatrix} [K_c]+[K_v]+[K_{f-s}] & -[K_{f-s}] \\ -[K_{f-s}] & [K_c]+[K_{f-s}] \end{bmatrix}\begin{Bmatrix} T_f \\ T_s \end{Bmatrix}$$

$$= \begin{Bmatrix} Q_{Q_f} \\ Q_{Q_s} \end{Bmatrix} \tag{12}$$

where $[K_c]$ is the conduction matrix, $[K_v]$ is the mass transport convection matrix, $[K_{f-s}]$ is the convection matrix between fluid and solid, $\{Q_Q\}$ is the internal heat generate load vector, $\{T_f\}$ and $\{T_s\}$ are the vectors of the nodal temperatures in the fluid and solid, respectively.

2.3 Adaptive Meshing

The basic idea of the adaptive meshing technique is to construct a completely new mesh based on the solution obtained from the previous mesh. The technique consists of two main steps; the first step is the determination of proper element sizes and the second step is the new mesh generation. The temperature, T, is used herein as the indicator for computing proper element sizes at different locations in the domain. As small elements must be placed in the region where changes in the temperature gradients are high, the second derivatives of the temperature at a point with respect to the global coordinates X and Y are needed. Using principal stresses determination from a given state of stresses at a point, the maximum principal quantities are then used to compute the proper element size h_i by requiring that the error should be uniform for all elements,

$$h_i^2 \lambda_i = h_{\min}^2 \lambda_{\max} = \text{constant} \tag{13}$$

where the subscript i denotes the direction of the maximum and minimum element length, and λ_i is the higher principal quantity of the element considered,

$$\lambda_i = \max\left(\left|\frac{\partial^2 T}{\partial X^2}\right|, \left|\frac{\partial^2 T}{\partial Y^2}\right|\right) \tag{14}$$

In Eq. (13), $\lambda_{\max}$ is the maximum principal quantity for all elements and $h_{\min}$ is the minimum element size specified by users. The node spacing, h_i, is scaled according to the maximum value of the second derivatives of the temperature. Such technique generates small elements in the regions with large change in the temperature gradients to increase the analysis solution accuracy. At the same time, larger elements are generated in the other regions where the temperature profile is nearly uniform to reduce the computational time and the computer memory.

3. Results

In this section two example problems are presented. The first example, a convectively-cooled solid subjected to uniform heating, is chosen to evaluate the nodeless variable finite element formulation and to validate the developed computer programs. The second example, a plate with intense heating, is used to evaluate the performance of the adaptive nodeless variable finite element method. The conjugate gradient method is used to solve the set of algebraic equations of these problems.

3.1 Convectively-cooled solid subjected to uniform heating

The first example for evaluating the efficiency of the nodeless variable finite element formulation is the problem of a convectively-cooled as shown in Fig. 1. The solid is subjected to uniform heating q along the upper wall. Heat is conducted in the solid and convection is occurred to the fluid that flows along the lower wall. All other walls of the solid are assumed to be adiabatic.

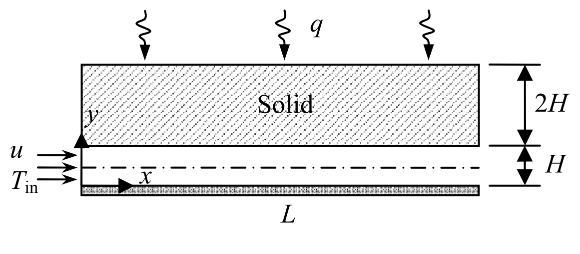

Figure 1. Problem statement of convectively-cooled solid subjected to uniform heating.

The parameters used in this example are as follows: the geometry sizes H = 0.1 m, L = 2 m, the uniform heating q = 8,000 W/m^2, the thermal conductivity k_s = 1,000 W/m-K, the flow channel parameters are Pe = 200 (Re = 286) and Pe = 400 (Re = 572) with Pr = 0.7. The convection coefficient, h is determined using the procedure presented in [10]. The finite element model consisting of 650 elements and 408 nodes, as shown in Fig. 2, is used in this study.

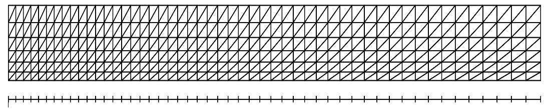

Figure 2. Nodeless variable finite element model consisting of 650 elements and 408 nodes.

Figure 3 shows the predicted temperature distributions along the upper wall, the lower wall and in the channel. The predicted temperature distributions in solid are shown in Fig. 4. Figure 5 shows the predicted temperature distributions at $x = L$, Pe = 200 for different conductivity ratios of K = k_s/k_f. The presented scheme is compared with the Navier-Stokes solution from Malatip et al. [5]. The figure shows good agreement of both the solutions.

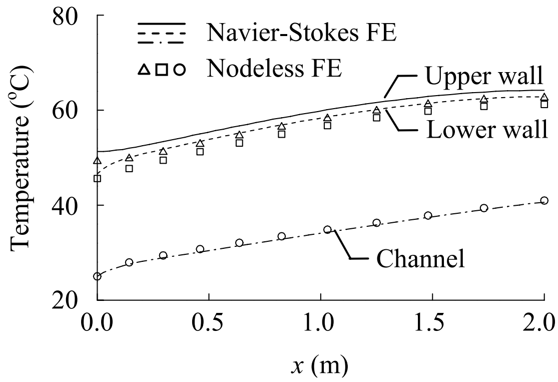

(a) Pe = 200

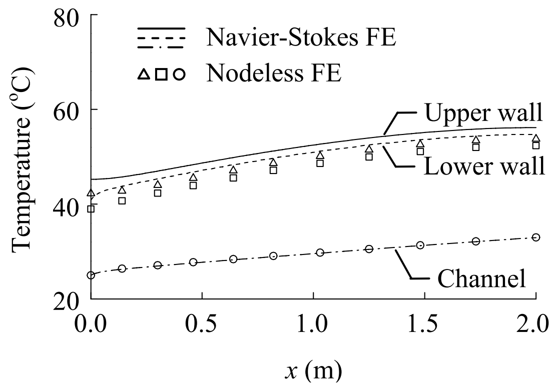

(b) Pe = 400

Figure 3. Comparative temperature distributions from the Navier-Stokes and nodeless variable finite element methods along the two walls and in the channel at (a) Pe = 200 and (b) Pe = 400.

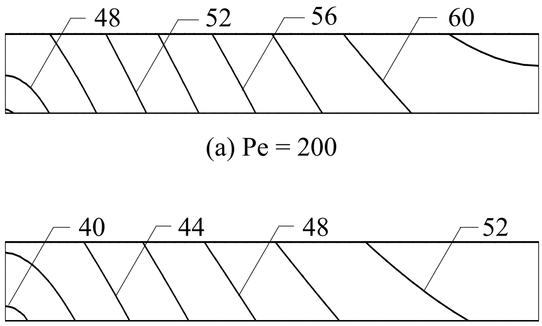

(a) Pe = 200

(b) Pe = 400

Figure 4. Predicted temperature contours from the nodeless variable finite element method at (a) Pe = 200 and (b) Pe = 400.

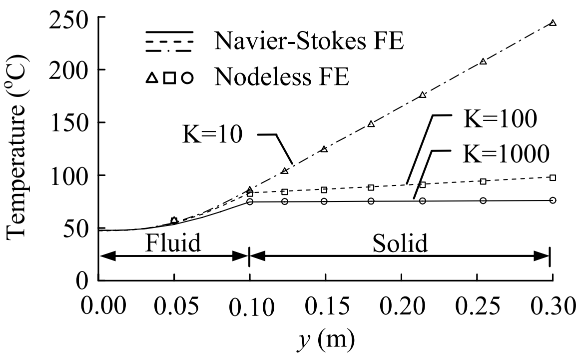

Figure 5. Comparative temperature distributions from the Navier-Stokes and nodeless variable finite element methods at $x = L$ and Pe = 200.

3.2 Plate with intense heating

To further evaluate the performance of the nodeless variable finite element method incorporated by the adaptive meshing technique, a plate subjected to intense heating is considered. The heating is simulated as a square width and the problem is considered into two cases. In the first case, the temperatures along the left, the right and the lower edges are constrained to zero. In the second case, convection heat transfer occurs from the lower edge of the plate to the fluid flow, while the left and the right edges are insulated.

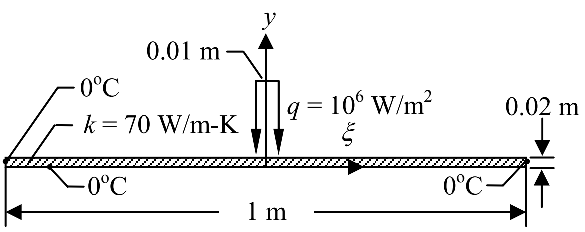

Figure 6. Problem statement of a plate subjected to intense heating.

In the first case as shown in Fig. 6, the exact plate temperature response can be calculated from [11],

$$T(\xi, y) = \frac{q}{Lk}\left\{ \sum_{n=2,4}^{\infty} \frac{1}{\lambda_n^3}\left[\sin\left(\frac{n\pi\xi}{2L}\right)\frac{\sinh(\lambda_n y)}{\cosh(\lambda_n H)}\right] + \sum_{n=1,3}^{\infty} \frac{1}{\lambda_n^3}\left[\frac{n\pi}{L}\sin(\alpha)\right] \left[\cos\left(\frac{n\pi\xi}{2L}\right)\frac{\sinh(\lambda_n y)}{\cosh(\lambda_n H)}\right]\right\} \tag{15}$$

where the origin of the ξ - y coordinate system is shown in Fig. 6, q is the heat source, H is the plate width, k is the plate thermal conductivity. The parameter α and λ_n in Eq. (15) are defined by

$$\alpha = \frac{n\pi w}{2L} \tag{16}$$

$$\lambda_n = \sqrt{\frac{n^2\pi^2}{4L^2}} \tag{17}$$

where L is the plate length, and w is the width of heat source.

Figure 7 shows a structured finite element mesh model consisting of 5600 elements and 3208 nodes, and an adaptive mesh model that consists of 742 elements and 446 nodes. Table 1 compares the predicted peak temperatures obtained from the two finite element meshes using the convectional and nodeless variable finite element methods. The values in the brackets denote the percentage errors of the peak temperatures as compared to the exact solution. Table 1 shows that the adaptive mesh uses fewer elements than the structured mesh but provides higher solution accuracy.

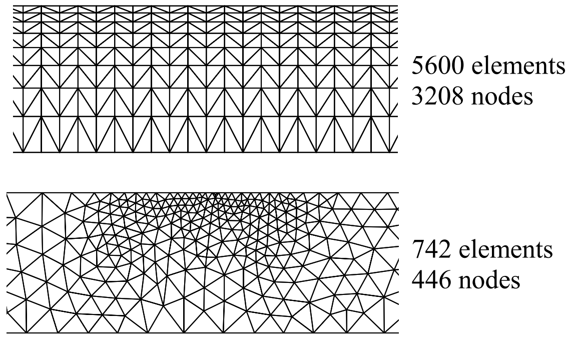

Figure 7. Structured and adaptive mesh models.

Figure 8 shows the adaptive mesh and the predicted temperature solution contours. Details of the adaptive mesh near the intense heating location and the temperature contours are shown in the lower figures. These figures show that small clustered elements are generated in the region of steep temperature gradients to capture the peak temperature and localized temperature distribution. At the same time, larger elements are generated in the other regions to reduce the computational time and the computer memory. The comparison of the exact and the predicted temperature distributions along the top edge is shown in Fig. 9. The figure shows that the temperature distribution obtained from the adaptive nodeless variable finite element method is in good agreement with the exact solution.

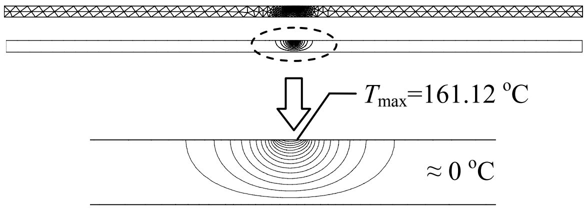

Figure 8. Adaptive mesh and the predicted temperature contours.

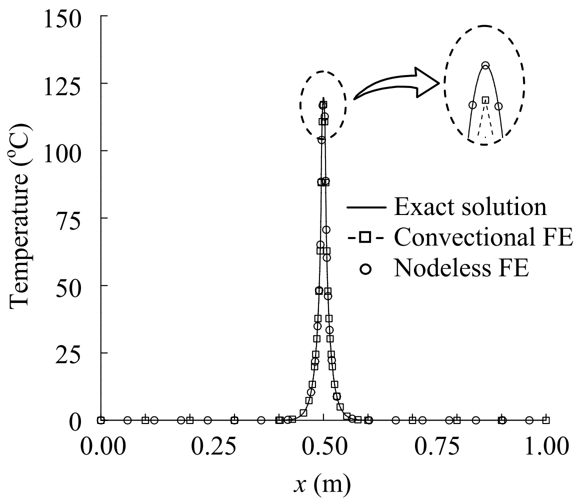

Figure 9. Comparison of the exact temperature and the predicted temperatures from the conventional method on structured mesh and the adaptive nodeless variable finite element methods.

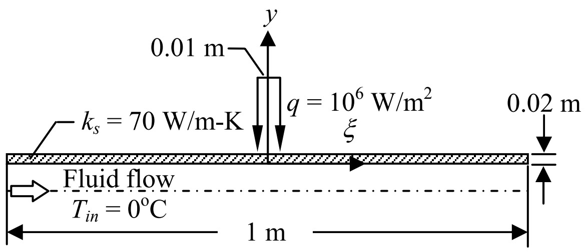

Figure 10. Problem statement of a convectively-cooled plate subjected to intense heating.

For the second case as shown by the problem statement in Fig. 10, a fully developed fluid flows beneath the lower edge of the plate while the other edges are insulated. The parameters of fluid used in the computation are as follows: the thermal conductivity k_f = 0.32 W/m-K, the specific heat c_f = 1,200 W/m-K, the density ρ = 54 kg/m^3, the mass flow rate $\dot{m}$ = 0.054 kg/s, the convection coefficient h = 929.52 W/m^2-k.

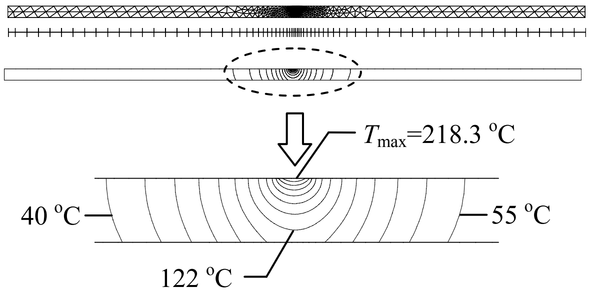

Figure 11. Adaptive mesh and the predicted temperature response for a convectively-cooled plate subjected to intense heating.

Figure 11 shows the adaptive mesh that consists of 1096 elements with 667 nodes and the predicted temperature contours. Details of the adaptive mesh near the intense heating location and the temperature contours are shown in the lower figures. At the heating location, the predicted peak temperatures are 218.30 °C and 217.91 °C from the nodeless variable and the conventional finite element methods. Figure 12 shows the temperature distributions along the top edge, the lower edge and in the channel obtained from the adaptive nodeless variable finite element method.

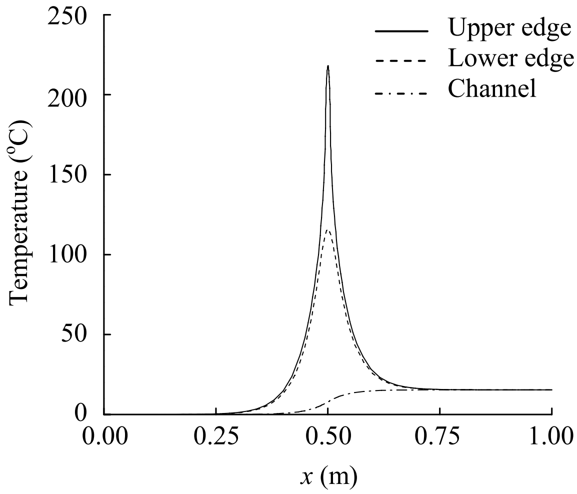

Figure 12. Predicted temperature distributions from the adaptive nodeless variable finite element method.

Table 1. Comparison of the predicted peak temperatures obtained from the conventional and the nodeless variable finite element methods on both the structured and adaptive meshes.

Mesh	Temperature (%Error)	
	Convectional FE	Nodeless FE
Structured	117.094 (2.169)	119.773 (0.070)
Adaptive	119.061 (0.526)	119.688 (0.002)

4. Conclusions

The adaptive nodeless variable finite element method for analysis of convectively-cooled solids was presented. The nodeless variable finite element is employed to improve the predicted solution without requiring actual nodes. The adaptive meshing technique was incorporated to reduce both the computer memory and computational time. Examples demonstrated that the adaptive nodeless variable finite element method can provide higher solution accuracy as compared to the conventional finite element technique.

5. Acknowledgement

The authors are pleased to acknowledge the Thailand Research Fund (TRF) for supporting this research work.

References

1. Thornton, E. A., and Dechaumphai, P., "Convective heat transport in merging flows" Third International Conference on Finite Elements in Water Resources, The University of Mississippi Oxford Campus, United States of America, 19-23 May 1980.
2. Wansophark, N., and Dechaumphai, P., 2002. Enhancement of Streamline Upwinding Finite Element Solution by Adaptive Meshing Technique. JSME International Journal, Vol. 45, No. 4, pp. 770-779.
3. Wansophark, N., and Dechaumphai, P., 2004. Combined Adaptive Meshing Technique and Segregated Finite Element Algorithm for Analysis of Free and Forced Convection Heat Transfer. Finite Elements in Analysis and Design, Vol. 40, pp. 645-663.
4. Thornton, E. A., and Dechaumphai, P., "Finite Element Analyses of Plane Thermal Entry-length Flows" Third International Conference on Finite Elements in Flow Problems, Banff, Alberta, Canada, 10-13 June 1980.
5. Malatip, A., Wansophark, N., and Dechaumphai, P., 2006. Combined Streamline Upwind Petrov Galerkin Method and Segregated Finite Element Algorithm for Conjugate Heat Transfer Problems. Journal of Mechanical Science and Technology, Vol. 20, No. 10, pp. 1741-1752.
6. Phongthanapanich, S., Traivivatana, S., Boonmaruth, P., and Dechaumphai, P., 2006. Nodeless Variable Finite Element Method for Heat Transfer Analysis by Means of Flux-Based Formulation and Mesh Adaption. Acta Mechanica Sinica, Vol. 22, No. 2, pp. 138-147.
7. Phongthanapanich, S., and Dechaumphai, P., 2008. Nodeless Variable Finite Element Method for Stress Analysis using Flux-Based Formulation. Journal of Mechanical Science and Technology, Vol. 22, No. 4, pp. 639-646.
8. Zienkiewicz, O. C., and Taylor, R. L., 2000. Finite Element Method, Volume 1, 5th ed. Butterworth-Heinemann, Woburn.
9. Huebner, K. A., Thornton, E. A., and Byrom, T. G., 1995. The Finite Element Method for Engineers, 3rd ed. John Wiley & Sons.
10. Kays, W. M, and Crawford, M. E., 1993. Convective Heat and Mass Transfer, 3rd ed. McGraw-Hill, Singapore.
11. McGowan, D. M., Carmarda, C. J., and Scotti, S. J., 1990. A Simplified Method of Thermal Analysis of a Cowl Leading Edge Subjected to Intense Localized Heating. NASA TP-16505.